A perceptive overview of nucleus-acoustic waves in degenerate quantum astroplasmas

Pralay Kumar Karmakar and Sayanti Dasgupta
Department of Physics, Tezpur University, Napaam-784028, Tezpur, Assam, India
E-mail: pkk@tezu.ernet.in

Abstract

We present a theoretic model formalism perspectively developed to explore the stability behavioral dynamics of the nucleus-acoustic waves (NAWs) in diversified gyrogravitating degenerate quantum astroplasmas. It evolves under the joint influence of the Bohm potential, Coriolis rotation, electrostatic confinement pressure (ECP), viscoelasticity, etc. Application of a standard normal spherical mode analysis yields a generalized linear septic dispersion law. It is interestingly found that the Coriolis rotation enhancement suppresses the NAW growth features. The adopted system is more sensitive to the rotational force than the viscoelasticity, and so forth. It is useful to study the NAWs and stability features excitable in compact astrophysical objects, like white dwarfs (WDs), brown dwarfs, neutron stars, etc.

1. Introduction

The area of quantum plasmas is one of the chief investigated fields of modern times, due to its large scale application in a broad spectrum, ranging from nano-to-astrophysical scales [1]. In astrophysical scales, quantum plasma occurs naturalistically in compact astrophysical objects, such as white dwarfs (WDs), brown dwarfs, neutron stars, etc [1, 2]. These WDs are actually the end products of stellar evolution for most of the low and medium mass main-sequence stars [2].

The study of nucleus-acoustic waves (NAWs) and instabilities in compact astrophysical objects has garnered attention since quite some time now. A good number of theoretic studies have also been conducted regarding the same [3-6]. The (heavy) NAWs here are the usual propagatory longitudinal oscillations excited by the conjugated interplay between the inertial force of the heavy nuclear species (HNS) and restoring force of the degenerate electronic species [4]. Several works have been reported in this explorative NAW direction set by both light nuclear species (LNS) and HNS [3-6].

Very recently, a semi-analytic theoretic study has been conducted using a quantum hydrodynamic model [5, 7, 8]. The multi-component plasma model comprises of degenerate electrons, LNS, and HNS [5]. It has reported the active influence of realistic plasma parameters on the growth characteristics of the linear NAWs in both the non-relativistic (NR) and ultra-relativistic (UR) regimes, and so forth [5]. The proposed work is a perceptive overview with a special foundation on a continued study of the same, but totally in new astronomical conditions. The model evolves amid the conjoint action of the quantum Bohm potential, Coriolis rotation force, electrostatic confinement pressure (ECP), viscoelasticity, and non-local self-gravity [5].

Apart from the brief introduction in Section 1, the basic model setup and dispersion relation are given in Section 2. Section 3 deals with the results and discussions, while Section 4 summarily concludes the main results, alongside correlations with actual astronomic evidences.

2. Basic model setup

We consider a gyrogravitating electrostatically confined quantum plasma system consisting of degenerate electrons, LNS, and HNS in a spherically symmetric geometry [5]. The dynamics of the system is modelled using the generalized quantum hydrodynamic model, by means of the flux conservation continuity equation, force-balancing momentum equation, and equation of state (EoS) for each of the three species [5]. The model is systematically closed with the help of electrostatic and self-gravitational Poisson equations. The electrons evolve under the simultaneous action of the electrostatic potential, electronic pressure (in both the NR and UR limits), and quantum Bohm potential [5]. The inertial and rotational force terms are ignored in the electronic momentum equation due to very small electronic mass [5]. The momentum equation of the classical weakly coupled LNS evolves dynamically under the influence of the forces arising by virtue of their motion, electrostatic potential, classical pressure (both thermal and ECP), and gravitational potential. The conjoint influence of the forces due to their motion, electrostatic potential, pressure (both thermal and ECP), non-local gravitational potential, viscoelasticity, and rotational force are retained in the momentum equation for the strongly-coupled HNS [5]. These equations are then normalized with a standard astronormalization scheme [3-5]. Application of a standard normal spherical mode analysis therein yields a generalized (Ω, k^*)-linear septic dispersion relation with atypical coefficients [5] cast as

$$\Omega^7 + A_6\Omega^6 + A_5\Omega^5 + A_4\Omega^4 + A_3\Omega^3 + A_2\Omega^2 + A_1\Omega + A_0 = 0\,; \quad (1)$$

$$A_6 = i\tau_m^{*-1}\,, \quad (2)$$

$$A_5 = \left\{\left(k^{*2} + \xi^{-2}\right)\left(1+\mu\beta\right)\left(-k^{*2} + F\right)^{-1} + \left(2E + Q - k^{*2}\chi^*\tau_m^{*-1}\right)\right\}\,, \quad (3)$$

$$A_4 = \left(i\tau_m^{*-1}\right)\left\{\left(k^{*2} + \xi^{-2}\right)\left(1+\mu\beta\right)\left(-k^{*2} + F\right)^{-1} + \left(2E+Q\right)\right\}\,, \quad (4)$$

$$A_3 = \Big[\mu\left(k^{*2} + \xi^{-2}\right)\left\{2E\beta - 2\sigma k^{*-2}\left(k^{*2} + \xi^{-2}\right) + E\mu^{-1}\right\}\left(-k^{*2} + F\right)^{-1} + \left\{2E + \left(k^{*2} + \xi^{-2}\right)\left(-k^{*2} + F\right)^{-1}\right\}\left(Q - k^{*2}\chi^*\tau_m^{*-1}\right) + \left\{E^2 - \mu\beta^{-1}\sigma^2 k^{*-4}\left(k^{*2} + \xi^{-2}\right)^2\right\}\Big]\,, \quad (5)$$

$$A_2 = \left(i\tau_m^{*-1}\right)\Big[\mu\left(k^{*2} + \xi^{-2}\right)\left\{2E\beta - 2\sigma k^{*-2}\left(k^{*2} + \xi^{-2}\right) + E\mu^{-1}\right\}\left(-k^{*2} + F\right)^{-1} + \left\{2E + \left(k^{*2} + \xi^{-2}\right)\left(-k^{*2} + F\right)^{-1}\right\}Q + \left\{E^2 - \mu\beta^{-1}\sigma^2 k^{*-4}\left(k^{*2} + \xi^{-2}\right)^2\right\}\Big]\,, \quad (6)$$

$$A_1 = \Big[\left(\mu\beta^{-1}\right)\left(k^{*2} + \xi^{-2}\right)\Big\{\beta^2E^2\left(-k^{*2} + F\right)^{-1} - \sigma k^{*-2} \times \left(k^{*2} + \xi^{-2}\right)\left(2\beta E\left(-k^{*2} + F\right)^{-1} + \sigma k^{*-2}E\right)\Big\} + \left\{E^2 + E\left(k^{*2} + \xi^{-2}\right)\left(-k^{*2} + F\right)^{-1}\right\} \times \left(Q - k^{*2}\chi^*\tau_m^{*-1}\right)\Big]\,, \quad (7)$$

$$A_0 = \left(i\tau_m^{*-1}\right)\Big[\left(\mu\beta^{-1}\right)\left(k^{*2} + \xi^{-2}\right)\Big\{\beta^2E^2\left(-k^{*2} + F\right)^{-1} - \sigma k^{*-2} + \left\{E^2 + E\left(k^{*2} + \xi^{-2}\right)\left(-k^{*2} + F\right)^{-1}\right\}Q\Big] \times \left(k^{*2} + \xi^{-2}\right)\left(2\beta E\left(-k^{*2} + F\right)^{-1} + \sigma k^{*-2}E\right)\Big\}\,. \quad (8)$$

Although Equation (1) could represent multiple modes excitable in the plasma system, we are interested in the extremely low-frequency one only. Accordingly, in the ultra-low frequency limit, Equation (1) simplifies as

$$\Omega = iP\left[\left\{\left(E^2\left(-k^{*2} + F\right) + E\left(k^{*2} + \frac{1}{\xi^2}\right) \times k^{*2}\chi^*\right\} - \tau_m^* P\right]^{-1}\,. \quad (9)$$

The various functional notations used are given as

$$E = \left(k^{*2} + \xi^{-2}\right)\left\{\sigma k^{*-2} - A_l'\left(T^* + 2B^*\right)\right\}; \quad (10)$$

$$F = \left(1+\mu\right)\left(0.25H'^2M_{Fe}^2k^{*2} - K'\gamma_e\right)^{-1}; \quad (11)$$

$$Q = \left[2C_F^*\left(ik^* + \xi^{-1}\right) + \left(k^{*2} + \xi^{-2}\right) \times \left\{\sigma k^{*-2}\mu\beta^{-1} - A_h'\left(T^* + 2C^*\right)\right\}\right]; \quad (12)$$

$$P = \Big[\left(\mu\beta^{-1}\right)\left(k^{*2} + \xi^{-2}\right)\left[\beta^2E - \sigma k^{*-2}\left(k^{*2} + \xi^{-2}\right) \times \left\{2\beta + \sigma k^{*-2}\left(-k^{*2} + F\right)\right\}\right] + \left\{E\left(-k^{*2} + F\right) + \left(k^{*2} + \xi^{-2}\right)\right\}Q\Big]. \quad (13)$$

Here, $\xi = r/\lambda_{Dl}$ is the normalized radial coordinate, the normalizing parameter, $\lambda_{Dl} = \left(m_ec^2/n_{l0}Z_le^2\right)^{1/2}$ is the plasma LNS Debye length. $\tau = t/\omega_{pl}^{-1}$ is the normalized time coordinate. $\tau_m^* = \tau_m/\omega_{pl}^{-1}$ is the normalized viscoelastic relaxation time. The time normalizing factor is the LNS oscillation time, $t_{pl} = \omega_{pl}^{-1} = \left(m_l/n_{l0}Z_l^2e^2\right)^{1/2}$. $\mu = Z_hn_{h0}/Z_ln_{l0}$ stands for the ratio of the equilibrium HNS-LNS charge densities. The relative nuclear charge-to-mass coupling parameter is given as $\beta = Z_h m_l/Z_l m_h$. The diverse population densities, $N_s = n_s/n_{s0}$, have been normalized with their respective equilibrium values. The Fermi Mach number is $M_{Fe} = v_{Fe}^2/cC_l$. Likewise, the normalized form of the fluid flow velocity is $M_s = u_s/C_l$, where $C_l = \left(Z_l m_ec^2/m_l\right)^{1/2}$ gives the rescaled light nuclear transit speed. $H' = \hbar\omega_{pl}/m_e v_{Fe}^2$ denotes the quantum parameter signifying the ratio between the plasmon energy associated with the light nucleus and the Fermi energy associated with degenerate electrons. The ratio between the square of the Jeans frequency $\omega_{Jl} = \sqrt{4\pi Gn_{l0}m_l}$ and the plasma oscillation frequency $\omega_{pl} = \left(n_{l0}Z_l^2e^2/m_l\right)^{1/2}$ is $\sigma = \omega_{Jl}^2/\omega_{pl}^2$. $A_l' = m_ec^2/m_l C_l^2$ stands for the ratio of the relativistic electron-to-LNS energy, $A_h' = m_ec^2/m_hC_l^2$ being its HNS counterpart. The constants *B* and *C* are normalized as $B^* = Bn_{l0}/m_ec^2$ and $C^* = Cn_{h0}/m_e c^2$, respectively. $T^* = k_BT/m_e c^2$ stands for the normalized isothermal nuclear plasma temperature. The effective generalized viscosity, $\chi = \left(\zeta + 4\eta/3\right)$, is similarly normalized as $\chi^* = \chi/m_h n_{h0}C_l\lambda_{Dl}$. The polytropic constant for the electronic species in the normalized form is given as $K' = K_e n_{e0}^{\gamma_e - 1}/m_ec^2$. The normalized Coriolis force is denoted as $C_F^* = \Omega_\phi^* M_{h\theta}$; the azimuthal and polar rotational components are normalized as $\Omega_\phi^* = \Omega_\phi/\omega_{pl}$ and $M_{h\theta} = v_\theta/C_l$, respectively. Then, $\Phi_E = e\Phi/m_ec^2$ gives the normalized electrostatic potential. The normalized gravitational potential is given as $\Psi = \psi/C_l^2$.

3. Results and discussions

A numerical illustrative platform is constructed to illustrate the NAW growth and stability features by means of the derived dispersion relation in the low-frequency regime (after Equation 9). It is for both the considered limits (NR+UR). The preliminary input data are taken from trustworthy literary sources [9-16]. It is to be noted that the data used here to obtain the profiles are strictly that of CO (carbon-oxygen) WDs [11, 12].

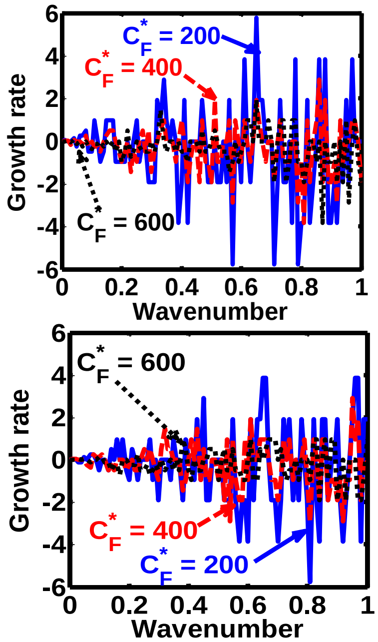

Figure 1. Profile of the normalized (rescaled) growth rate (Ω_i) with variation in the normalized angular wavenumber (k^*) in the (a) NR limit and (b) UR limit. The different lines link to $C_F^* = 200$ (blue solid), $C_F^* = 400$ (red dashed), and $C_F^* = 600$ (black dotted).

As in Figure 1, we depict the profile of the normalized growth rate $(\Omega_i$, rescaled with an auto-multiplicative factor, $10^{-34})$ with variation in the normalized angular wavenumber (k^*) for different indicated values of the normalized Coriolis rotational force (C_F^*). It is clearly seen that the Ω_i-peak occurs for $C_F^* = 200$, followed by $C_F^* = 400$ and $C_F^* = 600$, for both the NR-UR limits. The physical reason behind this can be attributed to the fact that the Coriolis force is dominant for the HNS, [$C_F = \left|\vec{F}_{Coriolis}\right| = -2 m_h v_{h,\theta} \Omega_\phi$]. As a consequence of this, it is clearly evident that higher Coriolis force means higher inertial force of the HNS, thereby suppressing the NAW growth features, and vice-versa.

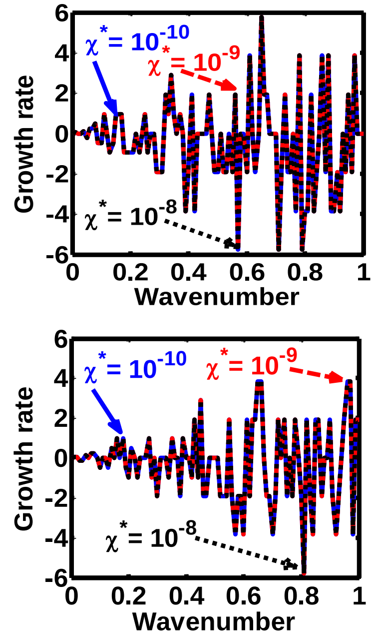

Figure 2. Same as Figure 1, but for different indicated values of the normalized effective generalized viscoelasticity (χ^*) in the (a) NR limit and (b) UR limit. The different lines link to $\chi^* = 10^{-8}$ (blue solid), $\chi^* = 10^{-9}$ (red dashed), and $\chi^* = 10^{-10}$ (black dotted).

In Figure 2, we depict the same as Figure 1, but for the different indicated values of the normalized effective generalized viscoelasticity (χ^*). It is clearly seen that, even though the plasma system responds to χ^*, it is not so sensitive to the χ^*-changes (Figure 2), as in the C_F^* variations (Figure 1). The microphysical reasoning behind this NAW behaviour may be the extreme small values of the considered viscoelastic force, and so forth.

In addition to the above, a common characteristic NAW growth feature in the form of intermittent irregularities is summarily speculated to exist in both the NR-UR regimes (Figures 1-2). The intermittency growth amplitude is more prominent towards the high-frequency (high-k^*) regime than the low-frequency (low-k^*) regime, and vice-versa. It happens because of the fact that higher frequency components in the NAW spectrum have more energy to undergo fluctuations than the corresponding lower spectral ones, and vice-versa.

On an important technological point, the NAW growth rate investigated here is in a normalized form rescaled with an auto-multiplicative factor of 10^{-34} (too small). It could be one of the possible explanations for the lack of astronomic discovery of the NAW growth signatures in compact astroobjects as of now. Besides, it is to be noted that a large number of non-radial pulsation modes have been discovered in PG1159 pre-WDs, variable DB (DBV), and variable DA [2]. This leads us to believe that there is a fair possibility for the discovery of the proposed NAWs in the near future, subject to astrometric advances and resolutional refinements.

4. Conclusions

A semi-analytic theoretic study, based on the lines of quantum hydrodynamics, is put forward to study the NAW stability features under the conjoint influence of the quantum Bohm potential, Coriolis rotation force, ECP, viscoelasticity, and self-gravity [5]. The proposed contribution is a continued exploration of the same, but in different astrophysical conditions. It is found mainly that a higher strength of the Coriolis rotational force lowers the NAW growth features, and vice-versa (Figure 1). It is further seen that the considered system is more sensitive to changes in the Coriolis force (Figure 1) as compared to the viscoelasticity case (Figure 2). An atypical intermittency pattern is speculated to exist in the NAW growth characteristics towards the high-frequency (high-k^*) regime against the low-frequency (low-k^*) spectral ones, and so forth.

It is to be admitted herewith that the presented model analysis has its own facts and faults. For an instance, a lack of exact data for some of the considered parametric factors could affect the accuracy of the desired results on the NAW stability behaviours. At the same time, the obtained NAW growth amplitudes are found to be relatively weaker. It is believed that a purely non-linear analysis (weak non-linearity treatment) to be conducted here would be highly beneficial in revealing important anti-linear NAW scenarios, but left for future study.

5. Acknowledgements

Active cooperation extended to us from our Tezpur University in different forms is deeply esteemed. The financial support received through the SERB Project (Grant- EMR / 2017 / 003222) is duly acknowledged.

6. References

[1] P. K. Shukla PK and B. Eliasson, “Nonlinear aspects of quantum plasma physics,” *Physics-Uspekhi*, **53**, 1, 2010, pp. 51-76, DOI: 10.3367/UFNe.0180.201001b.0055

[2] D. Koester, “White Dwarfs: Recent Developments,” *The Astronomy and Astrophysics Review*, **11**, 2002, pp. 33-66, DOI: 10.1007/s001590100015

[3] D. M. S. Zaman, M. Amina, P. R. Dip, and A. A. Mamun, “Planar and non-planar nucleus-acoustic shock structures in self-gravitating degenerate quantum plasma systems,” *European Physical Journal Plus*, **132**, 2017, pp. 457(1)-457(8), DOI 10.1140/epjp/i2017-11746-7

[4] P. K. Karmakar and P. Das, “Nucleus-acoustic waves: Excitation, propagation, and stability,” *Physics of Plasmas*, **25**, 2018, pp. 082902(1)-082902(7), https://doi.org/10.1063/1.5044610

[5] S. Dasgupta and P. K. Karmakar, “Propagatory dynamics of nucleus‑acoustic waves excited in gyrogravitating degenerate quantum plasmas electrostatically confined in curved geometry,” *Scientific Reports*, **11**, 2021, pp. 19126(1)-19126(12), https://doi.org/10.1038/s41598-021-98543-2

[6] S. Sultana, “Review of heavy‑nucleus‑acoustic nonlinear structures in cold degenerate plasmas,” *Reviews of Modern Plasma Physics*, **6**, 2022, pp. 6(1)-6(33), https://doi.org/10.1007/s41614-022-00067-3

[7] G. Manfredi, “How to model quantum plasmas,” arXiv:quant-ph/0505004, 2005, pp. 1-25.

[8] F. Haas, Quantum plasmas. An Hydrodynamic Approach, New York, Springer, 2011.

[9] S. Chandrasekhar, “The maximum mass of ideal white dwarfs,” *The Astrophysical Journal*, **74**, 1, July 1931, pp. 81-82, DOI: 10.1086/143324

[10] S. Chandrasekhar, “The density of white dwarf stars,” *Philosophical Magazine Series 7*, **11**, 70, 1931, pp. 592–596, https://doi.org/10.1080/14786443109461710

[11] K. R. Lang, Essential Astrophysics, Heidelberg, Springer, 2013.

[12] G. Fontaine, P. Brassard, and P. Bergeron, “The potential of white dwarf cosmochronology,” *Publications of the Astronomical Society of the Pacific*, **113**, 782, 2001, pp. 409-435, http://www.jstor.org/stable/10.1086/319535

[13] S. Dasgupta and P. K. Karmakar, “The Jeans instability in viscoelastic spherical astrophysical fluid media,” *Astrophysics and Space Science*, **364,** 2019, pp. 213(1)-213(7), https://doi.org/10.1007/s10509-019-3706-x

[14] M. K. Shukla and K. Avinash, “Equilibrium configuration of self-gravitating charged dust clouds: Particle approach,” *Physics of Plasmas*, **26**, 2019, pp. 013701(1)-013701(10), https://doi.org/10.1063/1.5053649

[15] M. K. Shukla, K. Avinash, R. Mukherjee, and R. Ganesh, “Isothermal Equation of State of Three Dimensional Yukawa Gas,” *Physics of Plasmas*, **24**, 2017, pp. 113704(1)-113704(6), https://doi.org/10.1063/1.5000409

[16] M. Livio and J. E. Pringle, “The rotation rates of white dwarfs and pulsars,” *The Astrophysical Journal*, **505**, 1998, pp. 339-343, DOI: 10.1086/306153